

# Toughening of bio-ceramics scaffolds by polymer coating

M. Peroglio<sup>a</sup>, L. Gremillard<sup>a</sup>, J. Chevalier<sup>a,\*</sup>,  
L. Chazeau<sup>a</sup>, C. Gauthier<sup>a</sup>, T. Hamaide<sup>b</sup>

<sup>a</sup> Materials Science Division (GEMPPM, UMR CNRS 5510), INSA Lyon, 20 Avenue Albert Einstein, 69621 Villeurbanne, France

<sup>b</sup> Laboratory for the Chemistry and Processes of Polymerisation (LCP, UMR CNRS 140), ESCPE Lyon,  
43 Bld du 11 Novembre 1918, 69616 Villeurbanne, France

Received 26 July 2006; accepted 18 October 2006

Available online 4 January 2007

## Abstract

In this work, polycaprolactone-coated alumina scaffolds were produced and characterized to validate the concept of polymer–ceramic composites with increased fracture resistance. Alumina scaffolds were sintered using a foam replication technique. An open-porous structure was achieved with ~70% porosity and 150  $\mu\text{m}$  mean pore size. The polymer coating was obtained by infiltrating the scaffold with either a polycaprolactone solution or a polycaprolactone nanodispersion. The latter was obtained by an emulsion–diffusion technique. Dynamical Young modulus measurements and four-point bending tests were conducted to evaluate the mechanical properties of the composites. It was found that their elastic behaviour is controlled on the first order by the ceramic scaffold, while the fracture energy mainly depends on the polymer phase. A 10–20 vol.% addition of polycaprolactone to alumina scaffolds led to a 7- to 13-fold increase of the apparent fracture energy. SEM observations showed that toughening is due to crack bridging by polymer fibrils.

© 2006 Elsevier Ltd. All rights reserved.

**Keywords:** Scaffold;  $\text{Al}_2\text{O}_3$ ; Composite; Mechanical properties

## 1. Introduction

Highly porous scaffolds with open structure are today the best candidates for cancellous bone substitution.<sup>1</sup> As compared to auto-grafts, synthetic bone substitutes involve less invasive surgery (a two step operation is necessary for the former) and are available in large quantities. As compared to xeno-grafts, the risk of rejection is much less important and the transmission of diseases is avoided.<sup>2</sup> Current synthetic scaffolds are processed from ceramic or polymer, but a better combination of mechanical and biological properties may be achieved with a composite or hybrid structure.

Many polymers have been proposed for medical applications,<sup>3</sup> either natural (collagen, alginate, glycosaminoglycan, starch, chitin and chitosan) or synthetic (poly(lactic acid), poly(glycolic acid), poly(hydroxybutyrate), poly( $\epsilon$ -caprolactone) (PCL), poly(ethylene oxide), poly(*p*-dioxanone), poly(methyl methacrylate), etc.).<sup>4</sup> Each of them presents differ-

ent biological and mechanical properties, allowing a choice of the right polymer for the right application. However, polymers usually present low modulus (below a few GPa) and creep resistance compared to bones (whose Young modulus ranges between 0.5 and 20 GPa depending on their type). This is the major reason that limits their clinical use for bone substitution.

Calcium phosphate ceramics (i.e. hydroxyapatite (HAP) and tricalcium phosphate (TCP)) and bioactive glasses (silica glasses containing calcium and phosphorus) have proven good biological properties and clinical successes in some specific applications (i.e. tibial osteotomy). However, calcium phosphates and bioactive glasses are brittle, impairing their use for load-bearing applications and making difficult the handling by the surgeon.

Using composites is a method to take advantage of both polymer and ceramics qualities, ideally to achieve materials with high stiffness and high toughness. Such composites can be based either on a polymer or a ceramic matrix and should be highly porous to meet the biological requirements for cancellous bone substitution.

The polymer matrix approach is the most widely studied, with a high number of systems proposed during the last

\* Corresponding author. Tel.: +33 4 72 43 61 25; fax: +33 4 72 43 85 28.  
E-mail address: [Jerome.chevalier@insa-lyon.fr](mailto:Jerome.chevalier@insa-lyon.fr) (J. Chevalier).

decades.<sup>5–8</sup> More recently, resorbable porous composite scaffolds constituted of PCL, PLA, polysulfone or their copolymers with additions of inorganic particles or fibres (mainly bioactive glass or hydroxyapatite) have been developed.<sup>9–14</sup> However, polymer matrix composites may not achieve the stiffness required for bone replacement, especially for load bearing regions.

A sintered ceramic scaffold will exhibit a higher stiffness and creep resistance than a ceramic-filled polymer of equivalent porosity. Nevertheless, the ceramic matrix route is much less studied. It consists in infiltrating a sintered ceramic scaffold with a polymer.<sup>15–17</sup> This approach is inspired by the fact that nearly 60 wt.% of dry bone is constituted by an inorganic phase (HAP). We believe that a mineral/organic ratio close that of natural bone will bring better integration of the bone substitute. Thus a material with high inorganic content may be preferred. The addition of a polymer phase to a ceramic scaffold is expected to enhance the resilience of the composite and to allow the functionalization of the surface.

Our long-term goal is therefore to process and characterize a new generation of tougher composite bone substitutes, made of a sintered ceramic scaffold infiltrated by a polymer phase. For this purpose, and as a first step, we propose to validate this concept with materials that are biocompatible but not optimized for bone substitution. Thus in this work, polycaprolactone-coated alumina scaffolds were produced and characterized. Alumina is a widely used material that finds applications in FDA approved bone graft devices; PCL is a biocompatible polymer exhibiting high fracture energy (compared to other biopolymers),<sup>5</sup> so it should give good toughening properties to the composite. PCL was processed in two different ways to achieve alumina scaffold infiltration: PCL solution in chloroform – which is easy to set up, fast and reproducible – and PCL nanodispersion in water – which avoids the use of organic solvents and is a more versatile method. The mechanical behaviour of the scaffolds was evaluated through four-point bending tests. Results are discussed in terms of both Young modulus and apparent fracture energy in relation with the microstructure.

## 2. Experimental

### 2.1. Alumina scaffolds

The alumina scaffolds were processed using a classical foam replication technique.<sup>18,19</sup> Alumina slurries were prepared in water from alumina powder (Ceralox SPA05) using a dispersant (Darvan C). Solid content of 75 wt.% (43 vol.%) was achieved. Different polymer foams were tested for infiltration and melamine foam (~250 ppi, Frina Mousse, France) was chosen because of its thin, needle like struts.<sup>20</sup> Pieces cut out of sheets of this melamine foam were infiltrated with controlled quantities of alumina slurry (the amount of slurry was calculated so that the porosity of the cellular ceramic after sintering would be 70%). The pieces were homogenised with a roller and left to dry at room temperature for at least 24 h. Samples were then heat-treated, first to remove the sacrificial melamine

scaffold (5 h at 600 °C, heating and cooling rate of 50 °C/h) and finally to sinter the alumina so as to obtain dense struts (1550 °C, 2 h30, heating and cooling rate of 300 °C/h).

Samples not undergoing further infiltration process will be later referred as “A”.

### 2.2. Infiltration with the polymer

#### 2.2.1. Infiltration with PCL solution

A 4 wt.% solution of PCL (Polycaprolactone, Aldrich,  $M_n = 80,000$  g/mol by SEC) in chloroform (Riedel-de-Haën, containing 1% ethanol) was chosen in order to obtain a viscosity (60 mPa s at a shear rate of  $500 \text{ s}^{-1}$ ) adequate for further infiltration of the ceramic scaffolds. Alumina porous scaffolds were outgassed and infiltrated in low vacuum conditions with the PCL solution. As infiltration was completed, the vacuum was released and evaporation of the solvent was held at ambient temperature for 2 days. After evaporation, differential scanning calorimetry (DSC) measurements were performed and demonstrated the lack of residual solvent. In order to increase the quantity of polymer in some scaffolds, the whole procedure was repeated and followed by a thermal treatment above and close to polymer melt temperature (80 °C, 70 min) to fuse the two PCL layers. Thereafter, samples with one PCL infiltration will be called “I”, “II” designating the samples with two infiltrations.

#### 2.2.2. Infiltration with PCL nanodispersion

A dispersion of PCL nanoparticles in water was prepared by an emulsification–diffusion technique, using a non-ionic surfactant (i.e. a triblock copolymer poly(ethylene oxide)-*b*-poly(propylene oxide)-*b*-poly(ethylene oxide): Pluronic F-68, Sigma). Detailed information on the dispersion technique can be found elsewhere.<sup>21,22</sup> Briefly, in a first step two solutions were prepared: a 2.5 wt.% PCL in water saturated ethyl acetate and a 4.5 wt.% Pluronic in ethyl acetate saturated water. The two solutions were then mixed (PCL/Pluronic weight ratio of 1/2) and emulsified with a sonicator (Bioblock Scientific, 750 W, 70% amplitude, 2 min). An important volume of deionized water (more than twice the volume of the emulsion) was added to the emulsion to create the gradient necessary to remove the ethyl acetate from the PCL nanoparticles. Finally, the nanodispersion was held at 80 °C under stirring until the desired concentration of particles was reached (8 wt.% solid content). Under these conditions, we obtained nanoparticles dispersed in water with a  $135 \pm 5$  nm mean size (as determined by Light Dynamic Diffusion, Malvern Zetasizer 3000).

Alumina samples were gradually covered with aqueous nanodispersion of PCL and evaporation was held at room temperature during 7 days. They were finally heated at 80 °C for 70 min in order to form a continuous film on the scaffolds. Alumina samples infiltrated with PCL nanoparticles will be called “IN”.

#### 2.2.3. Characterisation of the structure/microstructure

The structure of the different materials was investigated on fracture surfaces using scanning electron microscopes (SEM, Phillips XL20 and FEI XL30 ESEM FEG). The porosity was

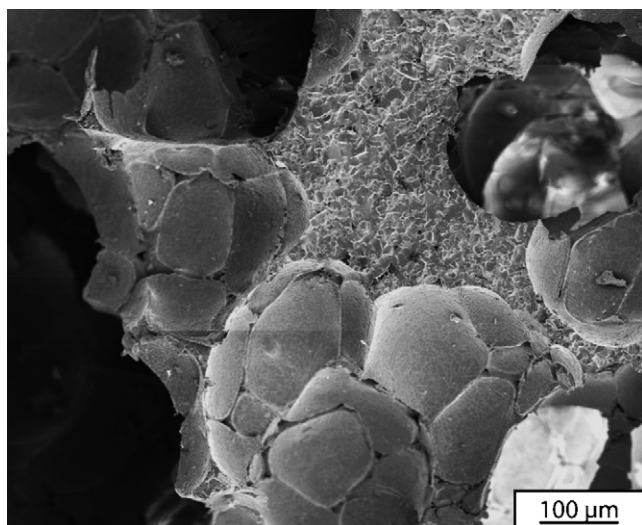


Fig. 1. Overall view of an alumina scaffold.

also characterized using mercury intrusion porosimetry (MIP, Micromeritics) using pressures ranging from 3.5 kPa to 400 MPa (corresponding to pore diameters ranging from 3 nm to 350 μm).

The apparent density of each sample was obtained from its weight and dimensions and compared when possible with values obtained from MIP.

#### 2.2.4. Mechanical characterisation

The Young modulus of each sample was measured using a dynamical method (Grindosonic®: the Young modulus is related to the natural frequency of the samples).

Samples were then collected in groups of seven to form four groups (A, I, II and IN) with similar Young modulus distributions. Four-point bending tests were conducted on 7 mm × 10 mm × 60 mm samples with an Instron universal testing machine at constant cross-head speed of 0.5 mm/min. The deflection and load were recorded during all tests. Apparent fracture energy was calculated for each sample by measuring the area under the load–deflection curve between 0 and 450 μm deflections (for infiltrated scaffolds, the tests had to be interrupted before fracture because the samples came in contact with the side of sample-holder).

### 3. Results

After sintering, alumina scaffolds with porosity ranging from 69% to 84% are obtained. The mean interconnection diameter measured by MIP is around 150 μm, which is high enough to allow very easy access of the cells to the volume of the material.<sup>11,23</sup> MIP does not detect the presence of open microporosity. Fig. 1 shows the overall structure of an alumina scaffold.

Infiltration of alumina scaffolds by PCL solutions gives satisfactory results since all the macro-pores are coated with a homogeneous layer of PCL (Fig. 2) and the infiltration process is reproducible. As expected, samples infiltrated twice contain a double quantity of polymer (26 vol.% of the porosity is occu-

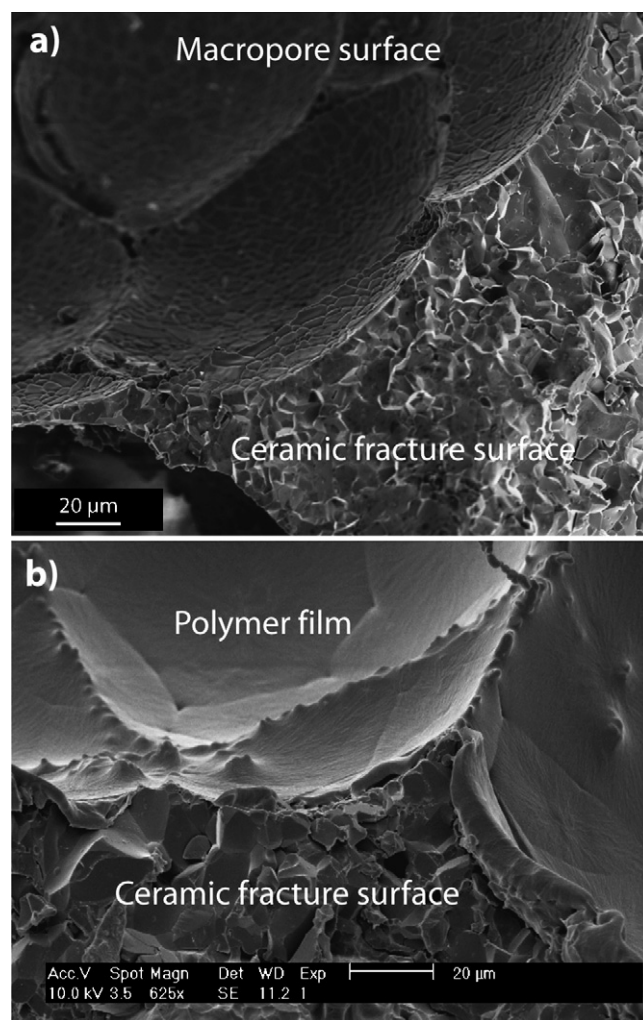


Fig. 2. Fracture surface of an alumina scaffold: (a) without infiltration and (b) infiltrated once (I) (note the homogeneous polycaprolactone coating).

pied by PCL in samples II, versus 13 vol.% in samples I), without losing homogeneity and reproducibility. Two infiltrations lead to a ~1/1 inorganic/organic volume ratio, which is similar to that of bone. Heat treatment leads to a uniform PCL phase: no interface can be distinguished by SEM between the first and the second layer.

Infiltration with nanoparticles leads to a polymer fraction in the scaffolds comparable to I samples (~13 vol.%). From SEM observations, it seems that the infiltration step followed by the drying sequence (7 days at room temperature) does not lead to a continuous PCL film and that nanoparticles remain distinct.

Young modulus of cellular alumina samples prior to infiltration ranges from 5 to 31 GPa with a standard deviation that can reach 35% of the mean modulus at a given density. These values are in the range of natural bone Young modulus. It is well correlated to the density, and follows approximately the Ashby equation for open-cell foams<sup>24</sup>:

$$E = E_0 \left( \frac{\rho_{\text{foam}}}{\rho_{\text{Alumina}}} \right)^2$$



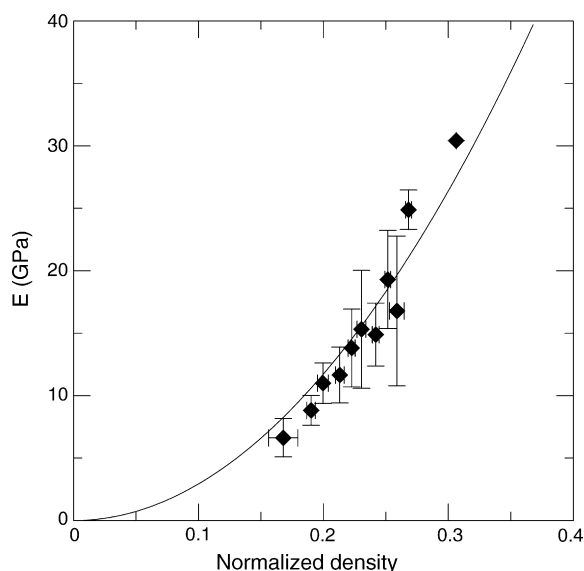


Fig. 3. Young modulus vs. normalized density of the pure alumina scaffolds (A). The continuous line is a fitting by Ashby open-cell foam model (with an alumina modulus of 280 GPa).

where  $E_0$  is the bulk modulus of alumina,  $E$  the modulus of the porous scaffold,  $\rho_{\text{Alumina}}$  the density of alumina and  $\rho_{\text{foam}}$  is the apparent density of the porous scaffold in spite of the wide variability (Fig. 3). The “bulk modulus” determined after Ashby model is  $E_0 = 280$  GPa, which is lower than the usual Young modulus for alumina (400 GPa). After infiltration with polycaprolactone, whatever the quantity or the infiltration technique no change in the Young modulus can be measured. This was expected since the Young modulus of polycaprolactone is negligible as compared to that of alumina.

During the four-point bending tests, pure alumina scaffolds exhibit a typical brittle, linear elastic behaviour. The tensile strength of these scaffolds ranges from 3.7 to 9.7 MPa, which is comparable to the values previously obtained for this kind of scaffolds.<sup>24</sup> Conversely to the prediction of Ashby,<sup>24</sup> the correlation between tensile strength and density is weak (Fig. 4). Even if a fit with Ashby model ( $\sigma_f = 0.2\sigma_{fs}(\rho_{\text{foam}}/\rho_{\text{Alumina}})^{3/2}$ , where  $\sigma_f$  is the fracture stress of the composite and  $\sigma_{fs}$  the strength of alumina struts) gives a correct value for the strength of the alumina struts (i.e. 257 MPa), the correlation coefficient is very low ( $r^2 \approx 0.23$ ).

More important, polycaprolactone addition completely changes the mechanical behaviour of the scaffold and the load–deflection curve can now be decomposed in three stages (Fig. 5). The initial stage exhibits a linear elastic behaviour. It is followed by a drop of the load, which leads to a plateau during which the load remains roughly constant while the deflection can reach several millimetres depending on the infiltration method. The plateau in the scaffolds infiltrated with nanoparticles is very short (generally less than 50  $\mu\text{m}$  of deflection) and at a very small load (around a tenth of the maximum load). On the other hand, the plateau in the scaffolds infiltrated with PCL solutions is much longer. We can only say that the deflection before final fracture is higher than 1 mm, since most of the tests had to be interrupted after a deflection of 1 mm because

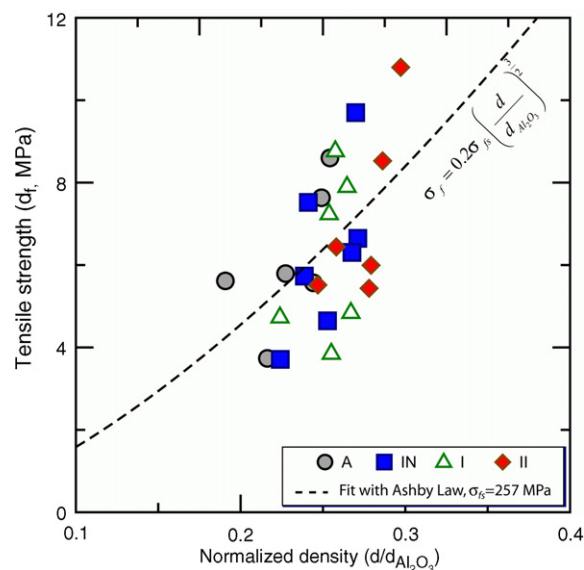


Fig. 4. Ultimate strength ( $\sigma_f$ ) vs. normalized density of the different scaffolds. The correlation is weak. Nevertheless, a fit with Ashby open-cell foam model gives a fracture strength of the struts ( $\sigma_{fs}$ ) of 257 MPa, coherent with the value measured on bulk alumina.

the samples came in contact with the side of the sample-holder. The level of the plateau depends on the quantity of PCL inside the scaffold: after one infiltration (corresponding to  $13 \pm 1\%$  of the pore volume occupied by PCL), the plateau is situated at one fourth of the maximum load (giving a seven-fold increase in the fracture energy) and after two infiltrations ( $25 \pm 3\%$  of the pore volume occupied by PCL) it is at half of the maximum load (fracture energy multiplied by 13 as compared with A samples). Fig. 6 shows the apparent fracture energy values of the different samples along with the quantity of polymer inside the pores.

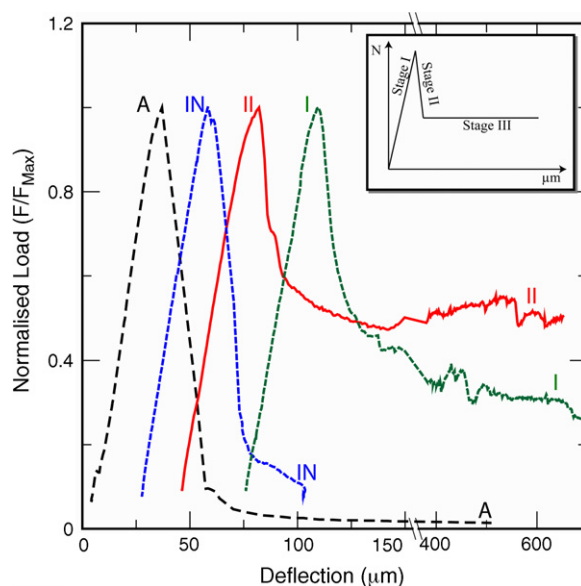


Fig. 5. Typical four-point bending load–deflection curves. The load was normalized to the maximum load to make the comparison more clear. Note the long load plateau for samples infiltrated with PCL solutions.

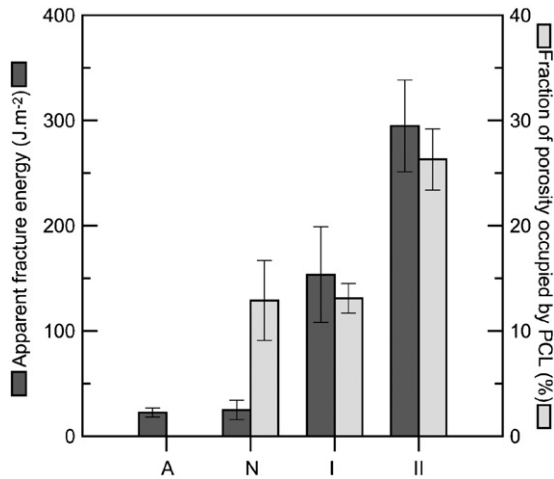


Fig. 6. Apparent fracture energy of the different samples alongside with the quantity of PCL in the porosities. Note the parallel evolution of these two parameters (except for the sample infiltrated with nanoparticles).

#### 4. Discussion

In the alumina samples, the better correlation of density with Young modulus than with strength can be explained by the structure heterogeneities created during the processing of the ceramic scaffold. Indeed, these heterogeneities are more important at high strain since they act as “weak points” for the initiation

of fracture. The fact that the modulus  $E_0$  found with Ashby’s equation is lower than expected is related to the technique used for its determination. Indeed, the Young modulus measured by dynamical method depends more on the percolation degree of the samples than on their density.

The significant improvement of mechanical properties (strain to fracture and apparent fracture energy) of the alumina-PCL materials can be explained very easily by examining the load–deflection curves presented in Fig. 5. For samples designated I and II, these curves show three different stages. The first stage is linear elastic, controlled at first order by the alumina scaffold alone. This is supported by the fact that Young modulus does not change with polymer addition, thus the elastic behaviour depends on the ceramic part only. In the second stage, we observe a drop of the load due to crack propagation in the alumina scaffold. In some cases the load drop is not brutal but progressive, indicating that some progressive damage occurs in the ceramic. In the third stage (the plateau) the load remains roughly constant while the deflection increases to several millimetres. Here, the ceramic scaffold is broken and the sample is held together by the PCL. As PCL is strained, crack opening leads to the formation of fibrils that bridge the crack in the ceramic, as shown in Fig. 7. The fibrils appear and develop in the zone of maximal tensile stress, i.e. of maximal crack opening displacement. Each fibril will progressively deform plastically before breaking as the crack opening displacement reaches a critical value. As a result, the zone of maximal tensile stress will

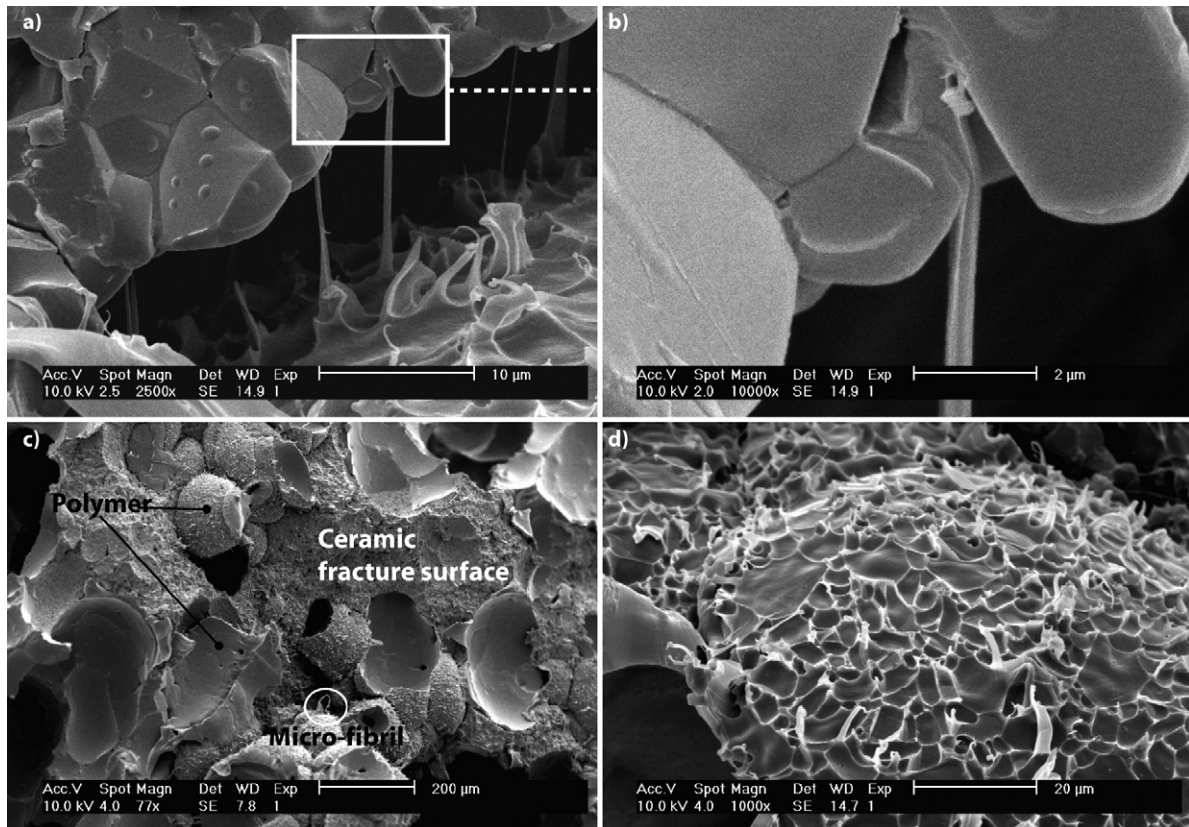


Fig. 7. Microstructure of a fractured polycaprolactone–alumina composite: (a) presence of PCL fibrils bridging the crack; (b) magnified view of a polycaprolactone fibril anchored to the alumina scaffold; (c) global view of the composite after fracture; (d) magnified view of the polycaprolactone coating after deformation and rupture showing high density of fibrils.

move progressively upward in the specimen stressing up new fibrils. Thus, the PCL phase controls the deformation to fracture. This hypothesis is supported by the fact that the plateau level depends on the quantity of polymer in the pores (more PCL means higher plateau—Fig. 5). The high deformation capability of PCL as compared to alumina explains the very high deformation prior final fracture of these materials.

It has been shown that one of the toughening mechanisms in bone is crack bridging by collagen fibrils.<sup>25</sup> Polycaprolactone fibrils seem to act in a similar way in alumina scaffolds. Moreover, the morphology of polycaprolactone fibrils (size, length and density) is very close to that observed for collagen fibrils in human bone.<sup>25</sup> The role of collagen in bone failure properties has been the subject of numerous studies. In a recent work, Currey<sup>26</sup> has shown that the post-yield strain of bone is highly dependent on collagen content. Degradation of collagen by irradiation makes bone more brittle, but does not affect the modulus of elasticity. The same feature is obtained with our scaffolds, infiltrated or not by polycaprolactone: Young modulus is unaffected by infiltration, but both post-yield strain and failure energy are greatly improved. These results are encouraging, even if only a combination with other toughening mechanisms observed in natural bone (i.e. micro-cracking, uncracked ligament bridging and crack deflection) will permit to approach human bone toughness.

The present results, obtained via the infiltration of ceramic scaffold with a polycaprolactone solution could probably be improved, in terms of height of the plateau, by adding more PCL in the scaffold. However, one must keep in mind the desired application, which is bone substitution. Indeed, the final materials have to meet at least two criteria: the cells responsible for bone reconstruction must have an easy access to all the porosities (which means that the interconnection size must not be smaller than 50  $\mu\text{m}$ ) and they must be able to interact with the ceramic part of the substitute (in real substitutes calcium phosphate or bioactive glass will provide an adequate surface for bone growth). Too much polymer in the material would certainly toughen the material, but might also decrease its biological activity.

Nanoparticle infiltrated samples (N) offer in contrast a disappointing mechanical behaviour. Indeed, no significant improvement is seen, although the quantity of polymer is equivalent in I and IN samples. We believe that the drying and filmification treatment did not lead to the formation of a continuous film but to a layer of juxtaposed particles without any chemical bonds between them. Optimisation of the drying sequence using higher temperature may be a way to improve the polymer interdiffusion and thus the coating quality. The formation of a continuous film would considerably increase the mechanical properties of scaffolds, the only limiting agent being a minimum dispersant content that could decrease the coherence of the polymer layer.

## 5. Conclusions

Highly porous materials made of a sintered alumina scaffold with open porosity coated with a polycaprolactone layer were elaborated. They exhibit the same stiffness as a pure alu-

mina scaffold, together with a fracture energy that can be 13 times higher. We show that the high fracture energy is due to the formation of PCL fibrils that bridge the cracks in the ceramic, leading to a plateau on the load–deflection curve.

Such an approach is applicable to other systems, for instance hydroxyapatite/polylactide that could be used for synthetic bone substitutes. An increase of the mechanical properties (strength and energy to fracture) of these bone substitutes would ease the handling and machining by the surgeon and even make possible the use of synthetic bone substitutes for load bearing applications without the help of invasive fixation devices.

## Acknowledgement

The authors wish to thank Ms. Tathiana Resnik, from Simon Bolivar University (Caracas, Venezuela) for her participation in this study.

## References

1. Tamai, N., Myoui, A., Tomita, T., Nakase, T., Tanaka, J., Ochi, T. *et al.*, Novel hydroxyapatite ceramics with an interconnective porous structure exhibit superior osteoconduction in vivo. *J. Biomed. Mater. Res.*, 2002, **59**, 110–117.
2. Bentz, R. R., Limitation of autograft and allograft: new synthetic solutions. *Orthopaedy*, 2002, **25**, 561–570.
3. Angelova, N. and Hunkeler, D., Rationalizing the design of polymeric biomaterials. *Trends Biotechnol.*, 1999, **17**, 409–421.
4. Ikada, Y. and Tsuji, H., Biodegradable polyesters for medical and ecological applications. *Macromol. Rapid Commun.*, 2000, **21**, 117–132.
5. Navarro, M., Ginebra, M. P., Planell, J. A., Barrias, C. C. and Barbosa, M. A., In vitro degradation behavior of a novel bioresorbable composite material based on PLA and a soluble CaP glass. *Acta Biomater.*, 2005, **1**, 411–419.
6. Chan, C., Thompson, I., Robinson, P., Wilson, J. and Hench, L., Evaluation of bioglass/dextran composite as a bone graft substitute. *Int. J. Oral Maxillofac. Surg.*, 2002, **31**, 73–77.
7. Mukherjee, D. P., Tunkle, A. S., Roberts, R. A., Clavenna, A., Rogers, S. and Smith, D., An animal evaluation of a paste of chitosan glutamate and hydroxyapatite as a synthetic bone graft material. *J. Biomed. Mater. Res. Pt. B: Appl. Biomater.*, 2003, **67B**, 603–609.
8. Ni, J. and Wang, M., In vitro evaluation of hydroxyapatite reinforced polyhydroxybutyrate composite. *Mater. Sci. Eng. C*, 2002, **20**, 101–109.
9. Marra, K. G., Szem, W. J., Kumta, P. N., DiMilla, P. A. and Weiss, L. E., In vitro analysis of biodegradable polymer blend/hydroxyapatite composites for bone tissue engineering. *J. Biomed. Mater. Res.*, 1999, **47**, 324–335.
10. Blaker, J. J., Maquet, V., Jérôme, R., Boccaccini, A. R. and Nazhat, S. N., Mechanical properties of highly porous PDLLA/Bioglass® composite foams as scaffolds for bone tissue engineering. *Acta Biomater.*, 2005, **1**, 643–652.
11. Hasegawa, S., Tamura, J., Neo, M., Goto, K., Shikunami, Y., Saito, M. *et al.*, In vivo evaluation of a porous hydroxyapatite/poly-DL-lactide composite for use as a bone substitute. *J. Biomed. Mater. Res.*, 2005, **75A**, 567–579.
12. Zhang, K., Ma, Y. and Francis, L. F., Porous polymer/bioactive glass composites for soft-to-hard tissue interfaces. *J. Biomed. Mater. Res.*, 2002, **61**, 551–563.
13. Roether, J. A., Gough, J. E., Boccaccini, A. R., Hench, L. L., Maquet, V. and Jérôme, R., Novel bioresorbable and bioactive composites based on bioactive glass and polylactide foams for bone tissue engineering. *J. Mater. Sci. Mater. Med.*, 2002, **13**, 1207–1214.
14. Niemelä, T., Niiranen, H., Kellomäki, M. and Törmälä, P., Self-reinforced composites of bioabsorbable polymer and bioactive glass with different bioactive glass contents. Part I: Initial mechanical properties and bioactivity. *Acta Biomater.*, 2005, **1**, 235–242.

15. Komlev, V. S., Barinov, S. M. and Rustichelli, F., Strength enhancement of porous hydroxyapatite ceramics by polymer infiltration. *J. Mater. Sci. Lett.*, 2003, **22**, 1215–1217.
16. Abdala, A. A., Milius, D. L., Adamson, D. H., Aksay, I. A. A. and Prud'homme, R. K., Inspired by abalone shell: strengthening of porous ceramics with polymers. *Polym. Mater.: Sci. Eng.*, 2004, **90**, 384–385.
17. Miao, X., Lim, W. K., Huang, X. and Chen, Y., Preparation and characterization of interpenetrating phased TCP/HA/PLGA composites. *Mater. Lett.*, 2005, **59**, 4000–4005.
18. Montanaro, L., Jorand, Y., Fantozzi, G. and Negro, A., Ceramic foams by powder processing. *J. Eur. Ceram. Soc.*, 1998, **18**, 1339–1350.
19. Innocentini, M. D. M., Sepulveda, P., Salvini, V. R. and Pandolfelli, V. C., Permeability and structure of cellular ceramics: a comparison between two preparation techniques. *J. Am. Ceram. Soc.*, 1998, **81**, 3349–3352.
20. Gremillard, L., Casadei, R., Saiz, E. and Tomsia, A. P., Elaboration of self-coating alumina based ceramics. *J. Mater. Sci.*, 2006, **41**, 5200–5207.
21. Quintanar-Guerrero, D., Fessi, H., Allemann, E. and Doelker, E., Influence of stabilizing agents and preparative variables on the formation of poly(D,L-lactic acid) nanoparticles by an emulsification–diffusion technique. *Int. J. Pharm.*, 1996, **143**, 133–141.
22. Quintanar-Guerrero, D., Allemann, E., Doelker, E. and Fessi, H., Preparation and characterization of nanocapsules from preformed polymers by a new process based on emulsification–diffusion technique. *Pharm. Res.*, 1998, **15**, 1056–1062.
23. Yang, S., Leong, K. F., Du, Z. and Chua, C. K., The design of scaffolds for use in tissue engineering. Part I: Traditional factors. *Tissue Eng.*, 2001, **7**, 679–689.
24. Gibson, L. J. and Ashby, M. F., In *Cellular solids, structure and properties*. 2nd ed. Cambridge University Press, Cambridge, United Kingdom, 1997.
25. Nalla, R. K., Kinney, J. H. and Ritchie, R. O., Mechanical fracture criteria for the failure of human cortical bone. *Nat. Mater.*, 2003, **2**, 164–168.
26. Currey, J. D., Role of collagen and other organics in the mechanical properties of bone. *Osteoporos. Int.*, 2003, **14**, S29–S36.